

# UC Irvine

## UC Irvine Previously Published Works

### Title

Impact of aircraft emissions on reactive nitrogen over the North Atlantic Flight Corridor region

### Permalink

<https://escholarship.org/uc/item/2wq625v2>

### Journal

Journal of Geophysical Research: Atmospheres, 105(D3)

### ISSN

0148-0227

### Authors

Koike, M  
Kondo, Y  
Ikeda, H  
[et al.](#)

### Publication Date

2000-02-16

### DOI

10.1029/1999jd901013

### Copyright Information

This work is made available under the terms of a Creative Commons Attribution License, available at <https://creativecommons.org/licenses/by/4.0/>

Peer reviewed

## Impact of aircraft emissions on reactive nitrogen over the North Atlantic Flight Corridor region

M. Koike,<sup>1</sup> Y. Kondo,<sup>1</sup> H. Ikeda,<sup>1</sup> G. L. Gregory,<sup>2</sup> B. E. Anderson,<sup>2</sup> G. W. Sachse,<sup>2</sup> D. R. Blake,<sup>3</sup> S. C. Liu,<sup>4</sup> H. B. Singh,<sup>5</sup> A. M. Thompson,<sup>6</sup> K. Kita,<sup>7</sup> Y. Zhao,<sup>1</sup> T. Sugita,<sup>8</sup> R. E. Shetter,<sup>9</sup> and N. Toriyama<sup>1</sup>

**Abstract.** The impact of aircraft emissions on reactive nitrogen in the upper troposphere (UT) and lowermost stratosphere (LS) was estimated using the  $\text{NO}_y$ - $\text{O}_3$  correlation obtained during the Subsonic Assessment (SASS) Ozone and Nitrogen Oxide Experiment (SONEX) carried out over the U.S. continent and North Atlantic Flight Corridor (NAFC) region in October and November 1997. To evaluate the large-scale impact, we made a reference  $\text{NO}_y$ - $\text{O}_3$  relationship in air masses, upon which aircraft emissions were considered to have little impact. For this purpose, the integrated input of  $\text{NO}_x$  from aircraft into an air mass along a 10-day back trajectory ( $\Delta\text{NO}_y$ ) was calculated based on the Abatement of Nuisance Caused by Air Traffic/European Commission (ANCAT/EC2) emission inventory. The excess  $\text{NO}_y$  ( $d\text{NO}_y$ ) was calculated from the observed  $\text{NO}_y$  and the reference  $\text{NO}_y$ - $\text{O}_3$  relationship. As a result, a weak positive correlation was found between the  $d\text{NO}_y$  and  $\Delta\text{NO}_y$ , and  $d\text{NO}_y$  and  $\text{NO}_x/\text{NO}_y$  values, while no positive correlation between the  $d\text{NO}_y$  and  $\text{CO}$  values was found, suggesting that  $d\text{NO}_y$  values can be used as a measure of the  $\text{NO}_x$  input from aircraft emissions. The excess  $\text{NO}_y$  values calculated from another  $\text{NO}_y$ - $\text{O}_3$  reference relationship made using in situ condensation nuclei data also agreed with these  $d\text{NO}_y$  values, within the uncertainties. At the NAFC region (45°N–60°N) the median value of  $d\text{NO}_y$  in the troposphere increased with altitude above 9 km and reached 70 parts per trillion by volume (pptv) (20% of  $\text{NO}_y$ ) at 11 km. The excess  $\text{NO}_x$  was estimated to be about half of the  $d\text{NO}_y$  values, corresponding to 30% of the observed  $\text{NO}_x$  level. Higher  $d\text{NO}_y$  values were generally found in air masses where  $\text{O}_3 = 75$ –125 ppbv, suggesting a more pronounced effect around the tropopause. The median value of  $d\text{NO}_y$  in the stratosphere at the NAFC region at 8.5–11.5 km was about 120 pptv. The higher  $d\text{NO}_y$  values in the LS were probably due to the accumulated effect of aircraft emissions, given the long residence time of affected air in the LS. Similar  $d\text{NO}_y$  values were also obtained in air masses sampled over the U.S. continent.

### 1. Introduction

Nitrogen oxide radicals ( $\text{NO}_x = \text{NO} + \text{NO}_2$ ) play a critical role in the photochemistry of ozone ( $\text{O}_3$ ) and hydrogen oxide radicals ( $\text{HO}_x = \text{OH} + \text{peroxy radicals}$ ) in the upper troposphere (UT) and lowermost stratosphere (LS). The major sources of total reactive nitrogen ( $\text{NO}_y = \text{NO} + \text{NO}_2 + \text{NO}_3 + \text{HNO}_2 + \text{HNO}_3 + \text{HNO}_4 + 2\text{N}_2\text{O}_5 + \text{peroxyacetyl nitrate (PAN)} + \text{other organic nitrates} + \text{aerosol nitrates}$ ) in

the UT are transport from the stratosphere,  $\text{NO}$  production by lightning, aircraft  $\text{NO}_x$  emissions, and convective transport of  $\text{NO}_y$ -rich air from the continental surface where  $\text{NO}_x$  is produced by fossil fuel combustion and other processes. According to three-dimensional (3-D) model calculations the contribution from each source is similar in magnitude at northern midlatitude UT during winter, while lightning becomes a major source in summer [Lamarque *et al.*, 1996]. Because of a rapid growth in air traffic in recent years, greater attention has been paid to the impact of aircraft  $\text{NO}_x$  emissions on the  $\text{O}_3$  chemistry in the UT and LS. Model calculations predict that aircraft emissions can have significant impact on large-scale  $\text{NO}_x$  distributions in the UT and LS in the northern midlatitudes and high latitudes [Brasseur *et al.*, 1996]. The emissions are especially extensive in the North Atlantic Flight Corridor (NAFC) region, where commercial air traffic is heavy at altitudes between 10 and 12 km [Baughcum *et al.*, 1996; Gardner, 1998]. The maximum increase in  $\text{NO}_x$  in the NAFC region was estimated to be between 50 and 90 parts per trillion by volume (pptv) at 200 hPa for July, based on several 3-D model calculations using a 1990 fleet of subsonic aircraft [Brasseur *et al.*, 1996, 1998, and references therein]. Sharp increases in  $\text{NO}_x$  concentrations within aircraft contrails were observed in the eastern NAFC region, and an aircraft source was successfully identified in some cases [Schlager *et al.*, 1997; Klemm *et al.*,

<sup>1</sup>Solar-Terrestrial Environment Laboratory, Nagoya University, Toyokawa, Japan.

<sup>2</sup>NASA Langley Research Center, Hampton, Virginia.

<sup>3</sup>Department of Chemistry, University California, Irvine.

<sup>4</sup>School of Earth and Atmospheric Sciences, Georgia Institute of Technology, Atlanta.

<sup>5</sup>NASA Ames Research Center, Moffett Field, California.

<sup>6</sup>NASA Goddard Space Flight Center, Greenbelt, Maryland.

<sup>7</sup>Department of Earth and Planetary Physics, Graduate School of Science, University of Tokyo, Tokyo, Japan.

<sup>8</sup>National Institute for Environmental Studies, Onogawa, Tsukuba, Japan.

<sup>9</sup>Atmospheric Chemistry Division, National Center for Atmospheric Research, Boulder, Colorado.

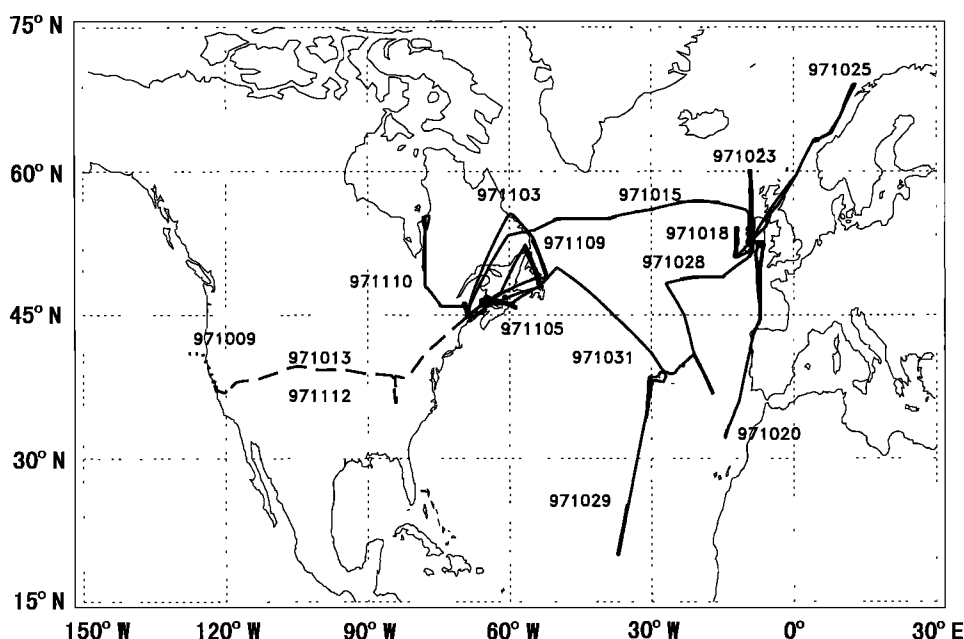


**Figure 1.** Flight tracks during the SONEX experiment. In this study, analyses were made in two study areas, the NAFC region at 45°N–60°N and 0°W–80°W (a part of flight tracks denoted by solid lines) and the region over the U.S. continent at 35°N–45°N and 70°W–120°W (dashed lines).

1998]. Although the large-scale effect (e.g., corridor effect) from aircraft emissions is more difficult to evaluate from the observation, a regional-scale enhancement in the  $\text{NO}/\text{NO}_y$  ratio was identified in the LS over the east coast of the U.S. continent by comparing the observed ratios with those of trajectory model calculations [Witte *et al.*, 1997].

The Subsonic Assessment (SASS) Ozone and Nitrogen Oxide Experiment (SONEX) was carried out using NASA's DC-8 aircraft in October and November 1997. Most of the aircraft measurements were made over the U.S. continent and the NAFC region (Figure 1). Four intensive flights were made from both Bangor, Maine (45°N, 68°W), and Shannon, Ireland (53°N, 9°W). A substantial amount of the data was obtained at altitudes between 8 and 11.5 km in both the UT and LS. Details of the experiment are described by Singh *et al.* [1999].

In this paper, the impact of aircraft emissions on the amount of reactive nitrogen was estimated using the  $\text{NO}_y$ - $\text{O}_3$  correlation. This is because a positive correlation between  $\text{NO}_y$  and  $\text{O}_3$  was generally observed in the UT and LS [Murphy *et al.*, 1993; Ridley *et al.*, 1994; Kondo *et al.*, 1996] and aircraft emissions can alter the correlation [Koike *et al.*, 1997]. In Plate 1 a correlation plot between  $\text{NO}_y$  and  $\text{O}_3$  using all of the 10-s SONEX data obtained above 8.5 km are shown. In this plate we excluded the data obtained within aircraft plumes, influenced by lightning, or affected by recent convective transport, as described in detail in the following section. As seen in this plate, the  $\text{NO}_y$  values at 45°N–60°N and those over the U.S. continent are generally higher than those obtained over the west coast of the United States and at 30°N–45°N and 60°N–70°N, where air traffic density is lower. As described in the following sections, a reference  $\text{NO}_y$ - $\text{O}_3$  relationship will be derived using data from air masses, in which aircraft emissions are considered to have little impact, that is, "background air." The excess  $\text{NO}_y$  ( $d\text{NO}_y$ ) will be estimated using this reference relationship. The statistical analyses of these  $d\text{NO}_y$  values will

be made for the data obtained at 45°N–60°N over the Atlantic (corresponding to the NAFC) and the U.S. continent. The excess  $\text{NO}_x$  ( $d\text{NO}_x$ ) will also be estimated using the reference  $\text{NO}_x/\text{NO}_y$  ratio in the background air.

## 2. Measurements and Data

### 2.1. Measurements

The  $\text{NO}$  and  $\text{NO}_y$  instrument used for SONEX was very similar to that used during NASA's Pacific Exploratory Mission West-B (PEM-West B) conducted in 1994 [Kondo *et al.*, 1997]. Both  $\text{NO}$  and  $\text{NO}_y$  were measured using a chemiluminescence technique.  $\text{NO}_y$  compounds were catalytically converted into  $\text{NO}$  on the surface of a heated gold tube with the addition of  $\text{CO}$ . The inlet tube for air sampling faced rearward discriminating against particles of diameter larger than about 1  $\mu\text{m}$ . The data were recorded every 1-s; however, 10-s averaged data were used in this study. The precision of the 10-s  $\text{NO}$  and  $\text{NO}_y$  measurements at 10 km estimated from the photon counts fluctuations ( $2\sigma$ ) was 6 and 19 pptv for  $\text{NO}$  and  $\text{NO}_y$ , values of 100 and 800 pptv, respectively. The absolute accuracy was estimated to be 8 and 10% for these  $\text{NO}$  and  $\text{NO}_y$  values.

During the SONEX experiment the same gold tube was used for all  $\text{NO}_y$  measurements. Other than operating the instrument using synthetic air, no attempt was made to clean the tube. The conversion efficiency of  $\text{NO}_2$  in ambient air was  $99 \pm 1\%$  during each flight. Possible interference in the  $\text{NO}_y$  measurements from the conversion of  $\text{HCN}$ ,  $\text{NH}_3$ , and  $\text{CH}_3\text{CN}$  was checked in the laboratory and during the flights. The conversion efficiency of  $\text{HCN}$  in dry synthetic air was between 0.5 and 4% on the ground before, during, and after the mission. It was also measured during the two test flights (at 6.4–11.9 km), using two independent  $\text{NO}_y$  channels and by adding a known amount of  $\text{HCN}$  gas into one of the channels. For one flight the conversion efficiency was  $2.1 \pm 0.5\%$  for the  $\text{O}_3$  and  $\text{H}_2\text{O}$

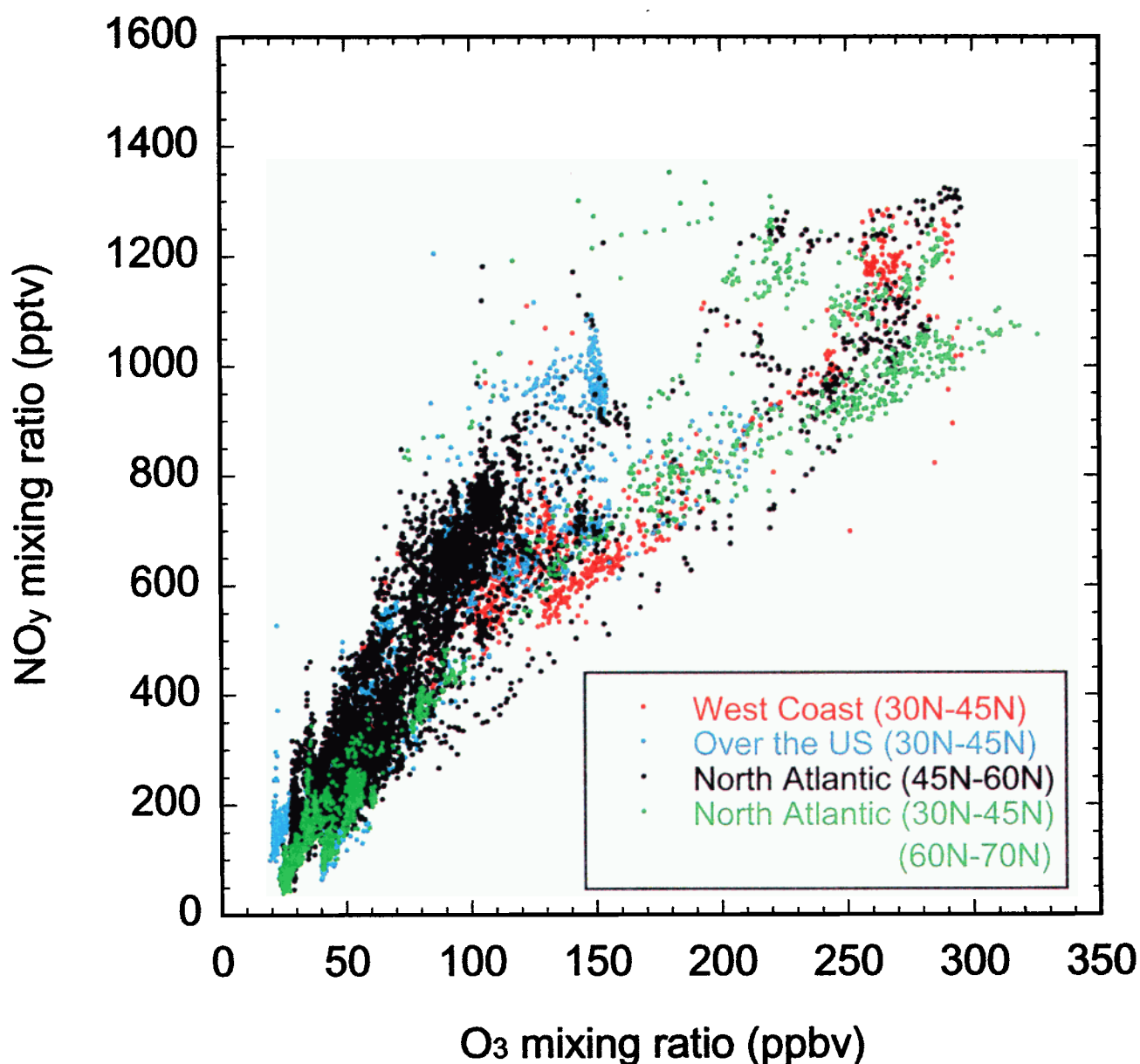


**Plate 1.** Correlation plot between NO<sub>y</sub> and O<sub>3</sub>. All SONEX 10-s data obtained above 8.5 km were used after excluding data obtained within aircraft plumes and data influenced by lightning or recent convective transport.

mixing ratios of 62–140 parts per billion by volume (ppbv) and 23–235 parts per million by volume (ppmv), respectively. For the other flight it was  $1.6 \pm 0.5\%$ , although the O<sub>3</sub> and H<sub>2</sub>O values were not measured. From these results, HCN was estimated to have contributed about 4 pptv to the SONEX NO<sub>y</sub> data assuming an average HCN mixing ratio of about 200 pptv [Rinsland *et al.*, 1982; Mahieu *et al.*, 1995]. The conversion efficiencies of NH<sub>3</sub> and CH<sub>3</sub>CN were also measured in the laboratory at 1–3 and 0.5–2%, respectively. Assuming mixing ratios of NH<sub>3</sub> and CH<sub>3</sub>CN in the UT of 1 pptv [Ziereis and Arnold, 1986] and 200 pptv [Hamm *et al.*, 1989], the interference from these species is considered to be negligible.

During the SONEX experiment the 15 s averaged actinic flux was measured using grating monochromators to calculate photolysis rates of NO<sub>2</sub> ( $J(\text{NO}_2)$ ) [Shetter and Müller, 1999]. The photostationary state NO<sub>2</sub>/NO ratios were calculated using the measured values of O<sub>3</sub>, temperature, pressure, and

$J(\text{NO}_2)$  for periods when the solar zenith angles were lower than 87°. The NO<sub>x</sub> mixing ratios were calculated from these NO<sub>2</sub>/NO ratios and the observed NO mixing ratios. The calculated NO<sub>2</sub>/NO ratios and NO<sub>x</sub> values were compared with those calculated using a box model in which a more complete photochemistry was included [Jaegle *et al.*, 1998]. At altitudes above 7 km they agreed within 30 and 10%, respectively. Simplified chemistry was used in this study to maximize the amount of NO<sub>x</sub> data.

In this study, 10-s averaged data of O<sub>3</sub>, N<sub>2</sub>O, and CO were also used. The O<sub>3</sub> measurements were made using a chemiluminescence technique, and N<sub>2</sub>O and CO were measured using a tunable diode laser system. The concentration of condensation nuclei (CN) with a diameter larger than 15 nm (CN fine particle; TSI model 3760) [Anderson *et al.*, 1999] was also used in this study. The unit of CN concentration was normalized to 0°C temperature and 1013 hPa (STP cm<sup>-3</sup>) to represent the

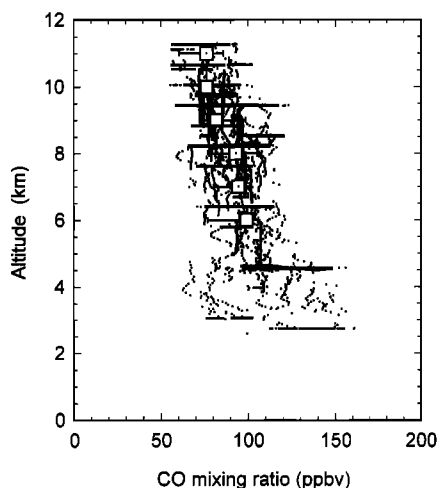


**Figure 2.** Vertical profile of CO using all the SONEX tropospheric data except for data from aircraft plumes and lightning events. Open squares and bars are median values and central 67% ranges in the NAFC region.

CN mixing ratio. Nonmethane hydrocarbons (NMHCs) and halocarbons were measured by collecting whole air samples and analyzing them using gas chromatography and flame ionization and electron capture detectors. The detection limit and sampling frequency of these measurements are summarized by Singh *et al.* [1999] and Simpson *et al.* [this issue].

## 2.2. Data Selection

During the SONEX experiment, most of the data were obtained at altitudes between 8 and 11.5 km. Air masses with  $\text{O}_3$  values lower and higher than 100 ppbv were defined as tropospheric and stratospheric, respectively. The stratospheric air masses were sampled at potential temperatures between 310 and 360 K, within the lowermost stratosphere (LS), the region above the midlatitude tropopause and below the isentrope touching the tropical tropopause, roughly 385 K, defined by Holton *et al.* [1995]. On the basis of the Microwave Temperature Profiler (MTP) tropopause height data the LS data were obtained within 2 km from the tropopause. The MTP data also showed that air masses with  $\text{O}_3$  values higher than 100 ppbv were sometimes obtained below the tropopause even though a clear signature of stratospheric air intrusion was not seen in the airborne differential absorption lidar (DIAL)  $\text{O}_3$  data. However, in general, air masses with  $\text{O}_3$  values higher than 100 ppbv were considered to have the same chemical characteristics as those from the LS. Similarly, air masses in which  $\text{O}_3$  values lower than 100 ppbv observed above the MTP-derived tropopause height were regarded as the UT ones.

In the present study, an increase in  $\text{NO}_x$  and  $\text{NO}_y$  from aircraft emissions was estimated for two study areas. The first area chosen was at latitudes between  $45^\circ\text{N}$  and  $60^\circ\text{N}$  and at longitudes between  $0^\circ\text{W}$  and  $80^\circ\text{W}$ . This data set was obtained mostly during the intensive flights from Bangor and Shannon (Figure 1). Air traffic density is quite high in this area and will be referred to as the “NAFC region” in the following. The other area was located over the U.S. continent at latitudes between  $35^\circ\text{N}$  and  $45^\circ\text{N}$  and at longitudes between  $70^\circ\text{W}$  and  $120^\circ\text{W}$ . The data set in this area was obtained during the two transit flights made on October 13, 1997, and November 12, 1997, between NASA Ames on the U.S. west coast and Bangor

on the east coast. This area will be referred to as the “U.S. continent region.”

When the measurements were made within the heavy air traffic region, sharp simultaneous increases in  $\text{NO}$  and  $\text{NO}_y$  values were often seen [Anderson *et al.*, 1999; T. Sugita *et al.*, manuscript in preparation, 1999]. These air masses were most likely sampled within aircraft plumes. The increase in the 1-s  $\text{NO}$  and  $\text{NO}_y$  data ranged from 100 pptv to a few ppbv. The time duration of the enhancement ranged from 1 to 60 s, with a median value of 4 s. Given the typical cruise speed of the NASA DC-8 aircraft of 200–250 m/s, the horizontal scales of the plumes were smaller than about 10 km with a typical size of about 1 km. On the basis of the Gaussian plume model, aircraft emission plumes are diluted to background concentrations within 5 to 10 hours for a typical wind shear condition with a corresponding horizontal size of 20 km [Schlager *et al.*, 1997; Gerz *et al.*, 1998]. Although the size of the  $\text{NO}_y$  enhancement observed from the NASA DC-8 depends on the geometry of the plume crossing, the maximum size of the observed plume was comparable to these estimates. These estimates were also consistent with a plume age of 10 min to 10 hours estimated using peak  $\text{NO}_y$  mixing ratios observed during SONEX [Anderson *et al.*, 1999]. In this study, the data obtained within the plumes were excluded in the evaluation of the large-scale impact from the aircraft emissions. This was because the sampling frequency of the plumes depends on the location and time of the measurement (many plumes were observed when the measurements were made in air masses just after heavy air traffic) and an inclusion of these data could be a potential cause of a bias in overestimating the aircraft impact. The excluded data corresponded to 6% of the entire data set at the 8.5 to 11.5 km altitude range. Because they were relatively infrequent, the results of this study would not change significantly even if the plumes were included in the analyses.

A clear signature of  $\text{NO}$  production by lightning was seen during four flights on October 13 and 29, 1997, and November 3 and 9, 1997 [Allen *et al.*, this issue; A. M. Thompson *et al.*, unpublished manuscript, 1999]. In these cases the  $\text{NO}_x$  and  $\text{NO}_y$  mixing ratios increased more than 1 ppbv, and  $\text{NO}_x/\text{NO}_y$  ratios ranged between 0.4 and 1.0 suggesting that  $\text{NO}$  production by lightning had occurred within a few days prior to the measurements. These results were generally consistent with air mass trajectory analysis, convective activities using cloud images, and lightning activities detected by the U.S. ground-based lightning network [Allen *et al.*, this issue; A. M. Thompson *et al.*, unpublished manuscript, 1999]. Possible influences from lightning were also observed on October 20 and 28, 1997. In this study all of the data likely to have been influenced by  $\text{NO}$  production by lightning were excluded. It should be noted, however, that the influence of lightning cannot be identified in an air mass once the  $\text{NO}_x$  in the air mass is diluted down near the background level. Consequently, we could not completely remove from our analysis the data which might have been affected by  $\text{NO}$  production from lightning. The contribution from lightning will be revisited in section 3.2.3.

The vertical profile of the CO in the troposphere is shown in Figure 2 using all of the data except for those obtained from aircraft plumes and clearly influenced by lightning. The median values and 67% ranges in the NAFC region are also shown. As seen in this figure, the CO mixing ratio generally decreased with altitude, and the median values were between 76 and 82 ppbv at 9 to 11 km. These values were systematically lower than the median CO values of 100 to 105 ppbv obtained in the

continental or maritime air masses in the UT over the middle to high latitude western Pacific in September and October [Kondo *et al.*, 1996]. In Figure 3 a correlation plot between NO<sub>y</sub> and CO is shown using the data obtained at altitudes above 8.5 km. Different symbols are used for the UT and LS data. The NO<sub>y</sub> mixing ratio did not generally have a positive correlation with the CO mixing ratio in the UT. These results suggest that NO<sub>y</sub> values in most of air masses in the UT obtained during SONEX had not been influenced by recent convective transport of polluted continental surface air. To eliminate the possible influence from recent convection, the data with CO values higher than 100 ppbv were excluded in this study. In addition, data showing a clear positive correlation between CO and NO<sub>y</sub> were also excluded. The excluded data by these criteria corresponded to 19% of the entire UT data set obtained above 8.5 km.

The correlations of NO<sub>y</sub> with nonmethane hydrocarbons such as ethyne (C<sub>2</sub>H<sub>2</sub>), ethane (C<sub>2</sub>H<sub>6</sub>), and propane (C<sub>3</sub>H<sub>8</sub>), and halocarbons such as tetrachloroethylene (C<sub>2</sub>Cl<sub>4</sub>), methyl iodide (CH<sub>3</sub>I), and CHBr<sub>3</sub> were also examined. No clear positive correlation was seen in the UT. In fact, NO<sub>y</sub> decreased with increasing mixing ratios of these hydrocarbons and halocarbons for NO<sub>y</sub> mixing ratios higher than 300 pptv (not shown). C<sub>2</sub>H<sub>2</sub>, C<sub>2</sub>H<sub>6</sub>, C<sub>3</sub>H<sub>8</sub>, and C<sub>2</sub>Cl<sub>4</sub> are emitted in urban areas. CH<sub>3</sub>I and CHBr<sub>3</sub> are considered to be good indicators of maritime air mass. The photochemical lifetimes of these species are comparable or shorter than that of CO. Consequently, the lack of a clear correlation of NO<sub>y</sub> with these species further confirms that the data selected in this study were generally free from the recent convective transport of air influenced by urban and other surface sources.

### 3. Results and Discussion

#### 3.1. Reference NO<sub>y</sub>-O<sub>3</sub> Relationship

To estimate the increase in the NO<sub>y</sub> mixing ratio due to aircraft emissions, we utilized a method that uses the NO<sub>y</sub>-O<sub>3</sub> relationship. In this method a reference NO<sub>y</sub>-O<sub>3</sub> relationship was estimated using data in air masses upon which aircraft emissions were believed to have had little impact, that is, "background air masses." To select the background air masses at 8.5–11.5 km, two independent approaches were taken. As described below, the agreement in the estimates on the excess NO<sub>y</sub> derived from these two approaches was evaluated, and the first approach described below was used for the further analyses.

For the first approach, 10-day back trajectories were calculated using a kinematic method for air masses sampled every 1 min on board the NASA DC-8. The European Centre for Medium-Range Weather Forecasts (ECMWF) data were used for this calculation. Then an integrated value of expected NO<sub>x</sub> input from aircraft emissions along each trajectory was calculated using the monthly mean values of the three-dimensional NO<sub>x</sub> emission distribution for October 1992, compiled in the Abatement of Nuisance Caused by Air Traffic/European Commission (ANCAT/EC2) emissions inventory [Gardner, 1998]. No chemical loss or diffusion process and no diurnal variation in the NO<sub>x</sub> emission rate were taken into account for this calculation, although some initial dilution effect was included because the emission rate was provided for each 1° × 1° in latitude and longitude and every 1 km in altitude. The typical emission rate in the corridor region was 2–5 pptv h<sup>-1</sup>. The calculated value is denoted as ΔNO<sub>y</sub>. For the present analysis,

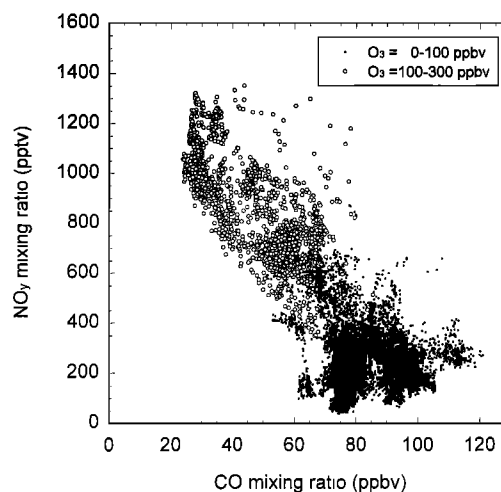


**Figure 3.** Correlation plot between NO<sub>y</sub> and CO. All the SONEX data at altitudes above 8.5 km were used except for the data from aircraft plumes and lightning events.

air masses in which the ΔNO<sub>y</sub> value was less than 40 pptv were used for the reference relationship irrespective of the location in which they were sampled. A large portion of the data in the O<sub>3</sub> = 100–200 ppbv range was obtained off the west coast of the United States (flight October 9, 1997). These air masses had been transported by westerly winds from locations over the Pacific Ocean where aircraft emissions are climatologically not very high. The data obtained at latitudes lower than 45°N and higher than 60°N were also selected as background for both the UT and LS. The criterion of 40 pptv within 10 days used in this study was admittedly arbitrary and subjective. A value of 40 pptv was chosen simply because enough data points in each O<sub>3</sub> range were selected by this criterion. However, the resultant estimates of aircraft effects were not very sensitive to the choice of this criterion as long as it was relatively small. If real background air masses were based on the criterion of ΔNO<sub>y</sub> = 0 pptv, the data selected under the present criterion would underestimate the aircraft impact. When 40 pptv was chosen as the criterion, 42 and 37% of the UT and LS air masses sampled above 8.5 km were classified as background air masses. In air masses when the ΔNO<sub>y</sub> values were lower or higher than 40 pptv, the median ΔNO<sub>y</sub> value was 17 or 100 pptv, respectively, in the UT, suggesting a large difference in the effect of aircraft on the two sets of air masses. The same feature was also seen in the LS where the median value of ΔNO<sub>y</sub> was 14 and 107 pptv. The median value of the NO<sub>y</sub> mixing ratio in the background air mass was then calculated for each 10 ppbv O<sub>3</sub> range, and a linear relationship was calculated using these median values in the UT and LS separately as shown in Figure 4. The relationships in the UT and LS were smoothly connected at the O<sub>3</sub> value of 100 ppbv. Using the reference NO<sub>y</sub>-O<sub>3</sub> relationship (referred as the "low ΔNO<sub>y</sub> reference" hereafter), the expected NO<sub>y</sub> value in the background air mass was calculated using the O<sub>3</sub> value simultaneously observed. The difference between this expected NO<sub>y</sub> value and the observed NO<sub>y</sub> value was defined as an excess NO<sub>y</sub> (dNO<sub>y</sub>).

For the second approach the CN concentration was chosen as the criterion. This is because within the plume of the aircraft, enhancements of the CN value were often observed simultaneously with enhancements of the NO and NO<sub>y</sub> [Anderson *et al.*, 1999]. Consequently, relatively higher CN

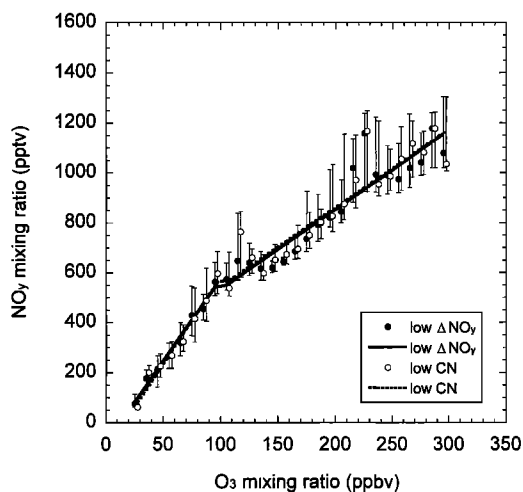


**Figure 4.** Two reference  $\text{NO}_y$ - $\text{O}_3$  relationships made using the background air masses obtained at altitudes between 8.5 and 11.5 km. The “low  $\Delta\text{NO}_y$ ” air masses received less than 40 pptv  $\text{NO}_x$  input from aircraft emission along the 10-day back trajectory based on the ANCAT/EC2 emission inventory. In the “low CN” air masses, CN concentration was less than 1500 or 1000  $\text{STP cm}^{-3}$  in the UT and LS, respectively. The bars indicate the central 67% range.

values can be expected when an air mass is influenced by aircraft emissions. As shown in Figure 5, the CN concentration increased with altitude both in the UT and LS. These vertical profiles could partly be due to aircraft emissions which are most intensive at altitudes between 10 and 12 km. In fact, the analysis made by Kondo *et al.* [1999] showed that the CN fine particle concentration positively correlated with the  $\text{NO}_x$  mixing ratio and  $\text{NO}_x/\text{NO}_y$  ratio in the LS air masses obtained during SONEX. Moreover, the slope of the positive correlation between the CN and  $\text{NO}_x$  values was generally close to the median value of the ratio between the enhanced levels of  $\text{NO}_y$  ( $\delta\text{NO}_y$ ) and CN ( $\delta\text{CN}$ ) found in the aircraft plumes ( $\delta\text{NO}_y/\delta\text{CN} = 0.11$  pptv  $\text{STP cm}^{-3}$ ). They concluded that an increase in CN particles due to aircraft emissions constituted 29% of the observed CN fine particle concentration. These results suggest

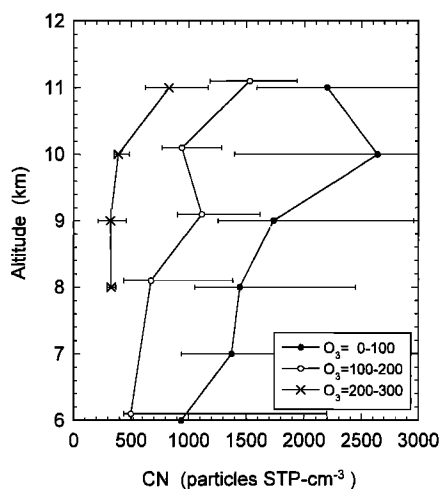


**Figure 5.** Vertical profile of the median values of the CN fine particle concentration in the NAFC region. The bars indicate the central 67% range. The  $\text{O}_3$  values are in units of ppbv.

that air masses with low CN values can be used as background in the LS. A positive correlation between the CN concentration and  $\text{NO}_x/\text{NO}_y$  ratio was also found in the UT in air masses with  $\text{CN} < 5000$   $\text{STP cm}^{-3}$  (Figure 6). Although the overall correlation was partly due to the vertical profile of CN and  $\text{NO}_x/\text{NO}_y$ , a positive correlation was generally found even within each 1 km layer and within limited  $\text{O}_3$  ranges. These results suggest that aircraft emissions played some role as a source of CN in the UT air masses sampled during SONEX. Using the SONEX data, Anderson *et al.* [1999] estimated that 8% of the CN fine particles in the northern hemispheric UT originated from aircraft emissions, based on the emission index of CN obtained within the aircraft plumes. However, it should be noted that when a clear enhancement of  $\text{NO}$  and  $\text{NO}_y$  due to lightning activity was seen during the above mentioned four flights, an enhancement of CN concentration up to  $3 \times 10^4$   $\text{STP cm}^{-3}$  was also seen. New particle formation in the cloud-scavenged air around cumulus clouds can elevate the CN concentration in the UT [e.g., Clarke *et al.*, 1998]. Consequently, although low CN air masses were considered to be relatively unaffected by aircraft emissions, high CN air masses were not necessarily affected greatly. For the present analysis, air masses with a CN concentration lower than 1500 and 1000  $\text{STP cm}^{-3}$  were used to make a reference  $\text{NO}_y$ - $\text{O}_3$  relationship in the UT and LS, respectively, irrespective of the location in which they were sampled. A different criterion was chosen because the CN concentration was systematically higher in the UT than in the LS (Figure 5). These data corresponded to 28 and 47% of the UT and LS data. As for the “low  $\Delta\text{NO}_y$  reference,” a median  $\text{NO}_y$  value was calculated for each 10 ppbv  $\text{O}_3$  range, and a linear relationship was calculated for the UT and LS data separately (Figure 4, denoted as the “low CN reference” hereafter). The  $d\text{NO}_y$  values were calculated for every 10-s data using this relationship. Note that data obtained from background air masses were not excluded and were used in conjunction with other data for the analyses described below.

It should be noted that products from three-dimensional

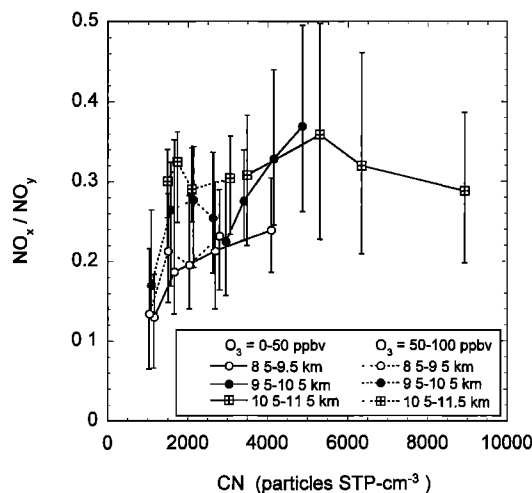


**Figure 6.** Correlation plot between  $\text{NO}_x/\text{NO}_y$  and CN fine particle concentration at three altitude ranges and two  $\text{O}_3$  ranges for air masses in the NAFC region. The data within each range were further divided into four subsets so that each subset contained the same amount of data. The median values and central 67% ranges were calculated for these subsets.

**Table 1.** Median Value of  $d\text{NO}_y$ 

	Reference 1 <sup>a</sup>		Reference 2 <sup>b</sup>	
	pptv	Percent	pptv	Percent
NAFC region				
Troposphere				
8.5–9.5 km	8 (–37~47)	3 (–15~17)	2 (–46~41)	1 (–19~15)
9.5–10.5 km	43 (–11~110)	16 (–4~34)	37 (–21~103)	13 (–7~32)
10.5–11.5 km	71 (–19~167)	21 (–6~35)	66 (–29~152)	18 (–10~34)
8.5–11.5 km	28 (–26~122)	11 (–10~29)	22 (–36~108)	8 (–13~28)
Stratosphere				
8.5–11.5 km	128 (–25~217)	16 (–3~27)	110 (–41~199)	14 (–5~25)
U.S. region				
Troposphere				
8.5–11.5 km	32 (–64~108)	11 (–35~39)	25 (–70~102)	9 (–39~40)
Stratosphere				
8.5–11.5 km	89 (3~294)	13 (0~31)	71 (–13~277)	10 (–2~29)

The central 67% ranges are shown in parentheses.

<sup>a</sup>Estimates using the low  $\Delta\text{NO}_y$  (model input  $\text{NO}_x$  value along 10-day back trajectory) reference.

<sup>b</sup>Estimates using the low CN reference.

chemistry transport models (CTMs) could also have been used to select the background air masses. However, this approach was not taken because the contribution from aircraft emissions was calculated in CTMs essentially in the same manner as was done in this study (i.e., the  $\Delta\text{NO}_y$  approach), while influences from convective transport and lightning observed in the UT were often not reproduced accurately by CTMs. An especially good agreement between CTMs and measurements at each point along the flight track of the DC-8 was required for the selection of the background air masses. Unfortunately, current CTMs do not have sufficient capabilities. Consequently, the use of CTM products would introduce an additional uncertainty in our estimates. It should also be noted that the criteria for selecting the background air masses were arbitrarily chosen in this study. However, even if CTM products had been used for the background air mass selection, we would still have had to choose some criteria on a subjective basis.

### 3.2. Validity and Uncertainty in the $d\text{NO}_y$ Estimate

**3.2.1. Reference values.** The median values of the  $d\text{NO}_y$  calculated using the two references are shown in Table 1 for both the UT and LS data. The median  $d\text{NO}_y$  values for each 1 km layer are also shown for the tropospheric data in the NAFC region (Figure 7). In this case, the  $d\text{NO}_y$  values were calculated down to 6.5 km, although the reference was derived using data from 8.5–11.5 km. The two sets of  $d\text{NO}_y$  values were generally in good agreement when relatively large uncertainties were considered. Because the two definitions of the background air mass had quite different characteristics, the agreement between the two sets of  $d\text{NO}_y$  values confirmed the validity of the method adopted in this study. The  $d\text{NO}_y$  values calculated using the low CN reference were slightly lower when compared to those calculated using the low  $\Delta\text{NO}_y$  reference. The median of the differences in the  $d\text{NO}_y$  values was 8 and 18 pptv in the UT and LS, respectively, suggesting the uncertainty in the  $d\text{NO}_y$  estimation caused by selecting the background air mass. Because the difference in the two sets of the  $d\text{NO}_y$  values was small and systematic, the values calculated from the low  $\Delta\text{NO}_y$  reference are used in the following discussion.

Although it is not shown here, similar results were also obtained when the  $d\text{NO}_y$  value was calculated using the  $\text{N}_2\text{O}$ – $\text{NO}_y$  relationship in the LS instead of using  $\text{NO}_y$ – $\text{O}_3$ .

**3.2.2. Correlation.** In Figure 8 a correlation plot between  $d\text{NO}_y$  and  $\Delta\text{NO}_y$  is shown for the UT NAFC data (8.5–11.5 km). In this figure the median  $d\text{NO}_y$  values for each 50 pptv range in the  $\Delta\text{NO}_y$  values and a one-to-one line are also shown. A large variability was generally seen in the  $d\text{NO}_y$  values presumably reflecting the wide variety of air mass histories. However, the median values of  $d\text{NO}_y$  generally increased with the  $\Delta\text{NO}_y$  values suggesting that the averaged  $d\text{NO}_y$  values were reasonable estimates for the aircraft impact on reactive nitrogen. The  $d\text{NO}_y$  values were generally lower than the  $\Delta\text{NO}_y$  values, partly due to the fact that when the  $\Delta\text{NO}_y$  value was higher, the  $\text{NO}_y$  value observed tended to decrease more because of dilution. On the other hand, the  $d\text{NO}_y$  value in the UT did not correlate with CO or  $\text{C}_2\text{H}_2$  in the NAFC and U.S. continent regions (not shown), suggesting that the high  $d\text{NO}_y$  values were generally not due to the convective transport of polluted air masses.

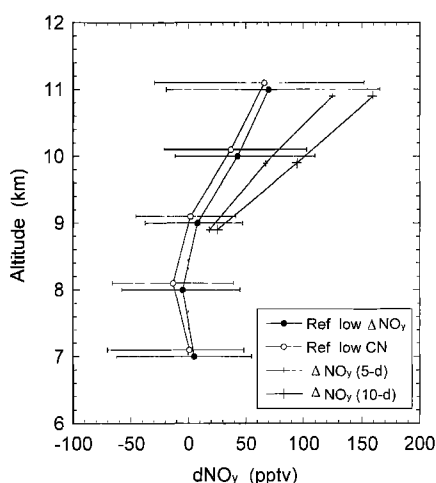


**Figure 7.** Vertical profile of the  $d\text{NO}_y$  values in the troposphere in the NAFC region calculated from the two reference  $\text{NO}_y$ – $\text{O}_3$  relationships. The median values and central 67% ranges are shown for each 1 km layer. The median values of the  $\Delta\text{NO}_y$  (integrated value of the model  $\text{NO}_x$  input along the 5- or 10-day back trajectory) are also plotted for the same air masses.



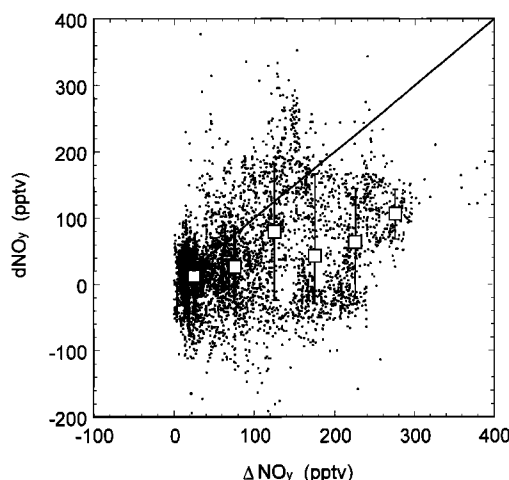


**Figure 8.** Correlation plot between  $d\text{NO}_y$  and  $\Delta\text{NO}_y$  (10 days) for air masses obtained in the UT (8.5–11.5 km) in the NAFC region. The median values and central 67% ranges are also shown for six  $\text{O}_3$  ranges. A one-to-one line is also shown.

**3.2.3. Influence from lightning.** One of the largest error sources, which can result in overestimating the  $d\text{NO}_y$  values in the UT, is influence from  $\text{NO}$  production by lightning. As described above, the data, which had a clear signature of  $\text{NO}$  production by lightning (i.e., distinct enhancement in the  $\text{NO}$  and  $\text{NO}_y$  mixing ratios and the  $\text{NO}_x/\text{NO}_y$  ratio), were excluded from the present analysis. However, these were the only cases in which data were removed showing the influence of recent  $\text{NO}$  production by lightning. Lightning activity generally has an effect similar to aircraft emissions: it increases the  $\text{NO}_x$  and  $\text{NO}_y$  mixing ratios, the  $\text{NO}_x/\text{NO}_y$  ratio, and the CN concentration. In order to estimate the effect of aircraft on air masses which had been minimally affected by lightning,  $d\text{NO}_y$  values were calculated using only air masses which had remained over the Atlantic Ocean more than 90% of time within 5 days prior to the measurements. This criterion was used because most lightning activities occur over land [e.g., Turman and Edgar, 1982]. In addition, air masses which had passed near the Florida Peninsula were also excluded because of the intensive lightning activity in that region. The selected data consisted of 27%

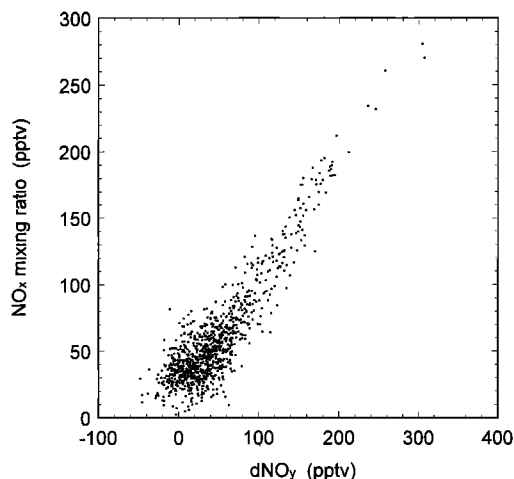


**Figure 9.** Correlation plot between  $\text{NO}_x$  and  $d\text{NO}_y$  for the flight made on October 23, 1997, at 8.5–11.5 km.

of the UT data in the NAFC region. As a result, the median  $d\text{NO}_y$  values in the 9.5–11.5 km range where the largest  $d\text{NO}_y$  values were obtained decreased by 24%. Because these air masses generally came from lower latitudes where aircraft  $\text{NO}_x$  emissions were lighter, the reduction in  $d\text{NO}_y$  values could also have been the result of the change in the effect of aircraft. However, this change in the  $d\text{NO}_y$  value provides an estimate of the degree of possible overestimation of the effect of aircraft in this study.

**3.2.4. Stagnated air mass within the NAFC region.** A clear indication that aircraft emissions had caused an increase in  $d\text{NO}_y$  was seen in air masses sampled during the flight made at the eastern NAFC region on October 23, 1997 (Figure 1). The correlation plot of  $\text{NO}_x$ - $d\text{NO}_y$  for this flight is shown in Figure 9. Most of the  $d\text{NO}_y$  was found to be in the form of  $\text{NO}_x$ , suggesting that the  $\text{NO}_x$  input had been made within the lifetime of  $\text{NO}_x$  of about 5 days (UT at 40°N–60°N). The 10-day back trajectories of the air masses obtained during this flight are shown in Figure 10. As shown in this figure, these air masses remained over the ocean at least 10 days and stagnated in the NAFC region the last 5 days. The median values of the  $\text{O}_3$  and  $\text{CO}$  mixing ratios in the UT (8.5–11.5 km) were 37 and 77 ppbv, and they changed little throughout the flight. Consequently, most of the change in  $\text{NO}_x$  and  $\text{NO}_y$  was quite likely due to aircraft emissions. The median and maximum values of the  $\Delta\text{NO}_y$  (10 days) were 71 and about 300 pptv, respectively, at altitudes between 9.5 and 11.5 km. Almost all of the input from aircraft was made within the last 5 days in this calculation. The median and maximum values of the  $d\text{NO}_y$  were 42 and about 200 pptv, respectively, in the 9.5–11.5 km altitude range. These data clearly indicate that aircraft emissions can raise the levels of  $\text{NO}_x$  and  $\text{NO}_y$  over a large region, and the effect was successfully detected by the method used in this study.

### 3.3. Vertical Profile of $d\text{NO}_y$

In the NAFC region of the troposphere, the  $d\text{NO}_y$  values were close to zero at altitudes between 7 and 9 km, suggesting minor impact from aircraft emissions (Figure 7). At altitudes above 9 km,  $d\text{NO}_y$  increased with altitude, reaching 43 and 71 pptv at 10 and 11 km, respectively. (37 and 66 pptv at these two altitudes when the low CN reference was used.) The medians

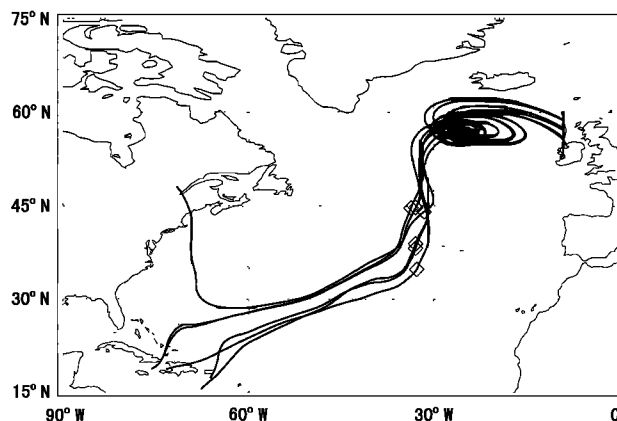


**Figure 10.** Ten-day back trajectory of air mass sampled in every 30 min between 0830 and 1100 UT during the flight made on October 23, 1997. Diamonds on the trajectories denote the location of air masses 5 days prior to the measurement.

of the  $d\text{NO}_y/\text{NO}_y$  ratio at these two altitudes were 16 and 21%; that is, about 20% of the NO<sub>y</sub> in the UT likely originated from aircraft emissions. These results are also summarized in Table 1.

As described above, the model input NO<sub>x</sub> value along the air mass trajectory,  $\Delta\text{NO}_y$ , was calculated for each data point. Consequently, a statistical analysis can be made on the  $\Delta\text{NO}_y$  value for the same data set from which the  $d\text{NO}_y$  values were calculated. In Figure 7 the median values of  $\Delta\text{NO}_y$  for the 5- and 10-day trajectories are shown. The median  $\Delta\text{NO}_y$  (10 days) was 25 pptv at 9 km and increased with altitude reaching 160 pptv at 11 km. The shape of the profile is consistent with that of the  $d\text{NO}_y$  value, although the  $d\text{NO}_y$  values were systematically lower than the  $\Delta\text{NO}_y$  values, a likely result of the dilution effect.

The median value of  $d\text{NO}_y$  in the UT over the U.S. continent region was calculated using all of the data obtained at 8.5–11.5 km range (Figure 11 and Table 1). This was because the amount of data was not sufficient to derive a vertical profile of the  $d\text{NO}_y$  values. The median value was 32 pptv, comparable to the 28 pptv in the NAFC region. Although the data over the U.S. continent were obtained from only two flights and the amount of data was smaller (4790 versus 1539 10-s data), the results here suggest a similar effect from aircraft emissions in the two regions.

The median value of  $d\text{NO}_y$  in the LS was calculated for the 8.5–11.5 km range (Figure 11 and Table 1). The median values of  $d\text{NO}_y$  and  $d\text{NO}_y/\text{NO}_y$  in the NAFC region were 128 pptv and 16%, respectively (110 pptv and 14% when the low CN reference was used.) The median  $d\text{NO}_y$  value over the U.S. continent region was 89 pptv, again comparable to the NAFC value when the large central 67% ranges are considered. It should be noted that these  $d\text{NO}_y$  values were systematically higher than those in the UT both in the NAFC and U.S. continent regions, 28 pptv versus 89 pptv in the NAFC region. The contrast in the  $d\text{NO}_y$  values between the UT and LS was much higher than that in the  $\Delta\text{NO}_y$  (10 days) values, at least in the NAFC region (72 pptv versus 102 pptv). One possible explanation is the longer residence time of NO<sub>y</sub> in the LS than in the UT. In the UT the NO<sub>y</sub> level can be lowered by dry and wet deposition of HNO<sub>3</sub> and aerosol nitrates through the vertical mixing of air. In the LS, NO<sub>y</sub> cannot be lost until the air mass is transported into the troposphere. Gettelman [1998] estimated the residence time was around 50 days for aircraft exhaust released in the lowermost stratosphere (LS) using the NASA 1992 zonal mean aircraft emission database. During SONEX all the stratospheric air masses were sampled in the LS as described above. Because the tropopause height was lower during late autumn, a larger amount of NO<sub>x</sub> could have been injected into the LS, and the LS air masses might have been influenced by the accumulated effect.

### 3.4. Relationship of $d\text{NO}_y$ With NO<sub>x</sub>/NO<sub>y</sub>, CN, and O<sub>3</sub>

In Figures 12a–12d the correlation plots between the  $d\text{NO}_y$  and NO<sub>x</sub>/NO<sub>y</sub> values and between the  $d\text{NO}_y$  and CN values are shown for the UT and LS using the data from both the NAFC and the U.S. continent regions. For these figures we used only the data in which the model input NO<sub>x</sub> values during the last 5 days were greater than 80% of the 10-day values (i.e.,  $\Delta\text{NO}_y$  (5 days)/ $\Delta\text{NO}_y$  (10 days) > 0.8). This is because NO<sub>x</sub> molecules emitted from aircraft more than 5 days prior to the measurements could have already been converted to higher oxidized species, such as HNO<sub>3</sub>. In fact, this data selection

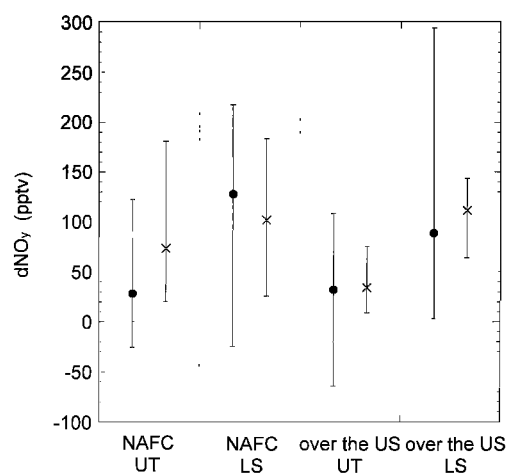


**Figure 11.** Median values and central 67% ranges of the values of  $d\text{NO}_y$  (solid circles) in the 8.5–11.5 km layer. The median values of  $\Delta\text{NO}_y$  (10 days) (crosses) are also shown.

generally improved the degree of correlation. The lifetime of NO<sub>x</sub> was estimated to be 4.8 and 3.2 days in the UT and LS ( $\text{O}_3 = 100\text{--}200$  ppbv), respectively, at 40°N–60°N using the observed values of aerosol surface area, etc. In Figure 12a the  $d\text{NO}_y$  values were plotted against the NO<sub>x</sub>/NO<sub>y</sub> ratios obtained in the UT. Different symbols were used for the data where  $\text{O}_3 = 0\text{--}50$  ppbv and  $50\text{--}100$  ppbv, respectively. The NO<sub>x</sub>/NO<sub>y</sub> ratio generally increased with  $d\text{NO}_y$  in both data sets. This is consistent with the fact that emissions of NO<sub>x</sub> from aircraft increases both the NO<sub>x</sub>/NO<sub>y</sub> ratio and  $d\text{NO}_y$  value. In other words, the change in the NO<sub>x</sub>/NO<sub>y</sub> ratio observed in the UT during SONEX was partly due to NO<sub>x</sub> from aircraft emissions. A positive correlation observed in the air masses where  $\text{O}_3 = 0\text{--}50$  ppbv was mostly due to those sampled on October 23, 1997, which had been strongly affected by aircraft emissions as described above. The degree of the NO<sub>x</sub>/NO<sub>y</sub> increase was higher for air masses where  $\text{O}_3 = 0\text{--}50$  ppbv than that for air masses where  $\text{O}_3 = 50\text{--}100$  ppbv when data with the same  $d\text{NO}_y$  value were compared. This result is plausible because the NO<sub>y</sub> value was generally lower when  $\text{O}_3$  was low (Plate 1) and the NO<sub>x</sub> input could cause a greater change in the NO<sub>x</sub>/NO<sub>y</sub> ratio.

In Figure 12b,  $d\text{NO}_y$  values are plotted against the CN concentration obtained in the UT. Kondo *et al.* [1999] and Anderson *et al.* [1999] calculated the ratio between enhanced levels of NO<sub>y</sub> ( $\delta\text{NO}_y$ ) and CN ( $\delta\text{CN}$ ) observed within aircraft plumes. The  $\delta\text{NO}_y/\delta\text{CN}$  ratio ranged between 0.04 and 0.2 pptv STP cm<sup>-3</sup> with a median value of 0.11 pptv STP cm<sup>-3</sup>. In Figure 12b, two lines having this slope and different intercepts are also plotted. As seen in this figure, the  $d\text{NO}_y$  value has a weak positive correlation with the CN concentration in both the air masses where  $\text{O}_3 = 0\text{--}50$  ppbv and  $50\text{--}100$  ppbv. On the basis of the passive cavity aerosol spectrometer probe (PCASP) measurements the median value of the aerosol surface area for aerosol particles with diameters between 0.1 and 3.0 μm was 1.7 μm<sup>2</sup> cm<sup>-3</sup> in the UT in the NAFC region. Under this condition, CN is lost primarily by the Brownian coagulation of CN, for CN concentrations higher than about 1400 STP cm<sup>-3</sup>. The half-lifetime of CN with a diameter of 15 nm at a CN concentration of 2500 STP cm<sup>-3</sup> is 1.3 days and decreases inversely with the CN mixing ratio [Pruppacher and Klett, 1997; B. Liley, personal communication 1999]. Because

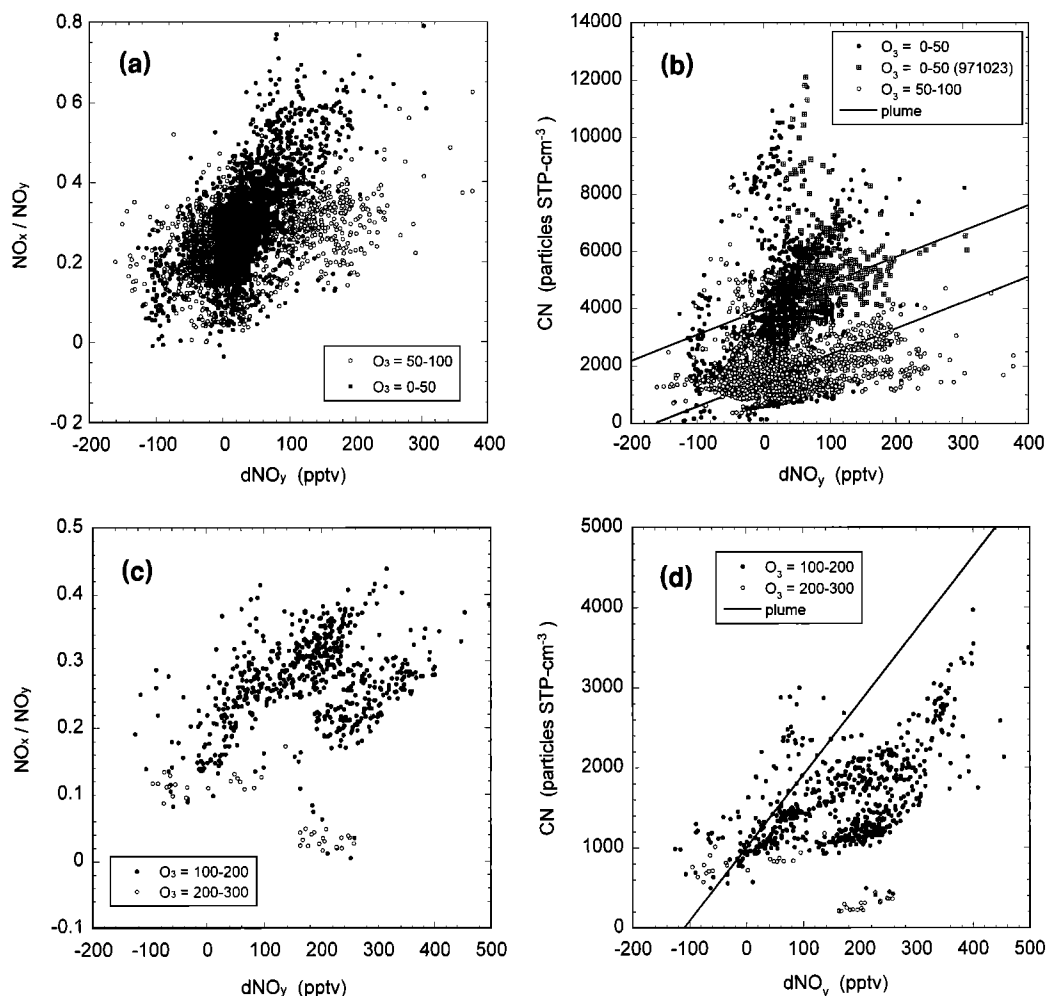


**Figure 12.** Correlation plot for  $\text{NO}_x/\text{NO}_y$ - $d\text{NO}_y$  and  $\text{CN}$ - $d\text{NO}_y$  in the UT and LS at altitudes of 8.5–11.5 km. The air masses obtained in both the NAFC and the U.S. continent regions were used. Only the air masses where  $\Delta\text{NO}_y$  (5 days)/ $\Delta\text{NO}_y$  (10 days)  $> 0.8$  were used. A slope of the median value of the ratio between the increase in  $\text{NO}_y$  and  $\text{CN}$  observed in aircraft plumes ( $\delta\text{NO}_y/\delta\text{CN} = 0.11$  pptv STP  $\text{cm}^3$ ) is also shown in Figures 12b and 12d. The data obtained on October 23, 1997, in air masses where  $\text{NO}_x > 60$  pptv are shown using a different symbol in Figure 12b. The  $\text{O}_3$  values are in units of ppbv.

the lifetime of  $\text{CN}$  was shorter than that of  $\text{NO}_x$  and  $\text{NO}_y$ , the  $\text{CN}$  concentration should be generally lower than that expected from the slope in the aircraft plumes if aircraft emissions were the dominant source of  $\text{CN}$ . Consequently, the observed result was not inconsistent with the hypothesis that aircraft emissions contributed to a source of  $\text{CN}$  for air masses where  $\text{O}_3 = 50$ – $100$  ppbv. On the other hand, other  $\text{CN}$  sources were predominant for air masses where  $\text{O}_3 = 0$ – $50$  ppbv because much higher  $\text{CN}$  concentrations than those expected from aircraft emissions were observed in these air masses. In fact, no correlation between  $\text{CN}$  and  $\text{NO}_x/\text{NO}_y$  was found for air masses where  $\text{CN} > 5000$  STP  $\text{cm}^{-3}$  as described above (Figure 6). However, it should be noted that a positive correlation having a similar slope to that within the aircraft plumes was seen in some air masses. As described above, air masses sampled on October 23, 1997, had probably been strongly affected by aircraft emissions (see subsection 3.2.4), and the  $\text{O}_3$  values in these air masses were mostly below 50 ppbv. The data where  $\text{NO}_x$  was higher than 60 pptv obtained on this day are shown using a different symbol in Figure 12b, and their  $\text{CN}$ - $d\text{NO}_y$  slope was found to be generally similar to that observed within

the aircraft plumes. Consequently, aircraft emissions could have caused an increase in the  $\text{CN}$  concentration in the UT in some cases during SONEX, resulting in the positive correlation between  $\text{CN}$  and  $d\text{NO}_y$ , and  $\text{CN}$  and  $\text{NO}_x/\text{NO}_y$ , although the background level of the  $\text{CN}$  concentration was changed greatly by other  $\text{CN}$  sources.

In Figure 12c the correlation plot between  $d\text{NO}_y$  and the  $\text{NO}_x/\text{NO}_y$  ratio in the LS is shown. A positive correlation was generally found in the LS. Because the LS air mass was generally free from tropospheric reactive nitrogen sources, the results shown here strongly suggest that an  $\text{NO}_x$  input from aircraft emissions primarily caused the  $\text{NO}_x$  variation in the LS.

In Figure 12d the correlation plot between  $d\text{NO}_y$  and  $\text{CN}$  in the LS is shown. A clear positive correlation between the two parameters was found suggesting that aircraft emissions were an important source of  $\text{CN}$  in the LS. The slope between  $d\text{NO}_y$  and  $\text{CN}$  was generally smaller as compared to the median  $\delta\text{NO}_y/\delta\text{CN}$  ratio of 0.11 pptv STP  $\text{cm}^3$  observed in aircraft plumes. This is reasonable because the lifetime of  $\text{NO}_y$  is much longer than that of  $\text{CN}$  in the LS.

In Figures 13a and 13b the correlation plots between  $d\text{NO}_y$  and  $\text{O}_3$ , and  $\text{NO}_x/\text{NO}_y$  and  $\text{O}_3$ , are shown using both the UT and LS data in the NAFC region. The median values of  $d\text{NO}_y$  or  $\text{NO}_x/\text{NO}_y$  in seven  $\text{O}_3$  ranges are also shown. Systematically large  $d\text{NO}_y$  values were generally found with  $\text{O}_3$  values between 75 and 125 ppbv. The  $d\text{NO}_y$  values were generally distributed around zero for lower and higher  $\text{O}_3$  air masses. These features are quite similar to those of the correlation plot between  $\text{NO}_x/\text{NO}_y$  and  $\text{O}_3$ , suggesting a relatively greater effect from aircraft emissions in the air masses with  $\text{O}_3$  values between 75 and 125 ppbv. These air masses likely remained around the tropopause altitude where  $\text{NO}_x$  input from aircraft emissions is large. Air masses with a lower  $\text{O}_3$  mixing ratio in the UT could generally be more strongly influenced by lower-altitude air. This is consistent with the fact that the  $d\text{NO}_y$  values were close to zero when the CO and  $\text{C}_2\text{H}_2$  values were high. Similarly, air masses with  $\text{O}_3$  values higher than 125 ppbv are considered to be less affected by aircraft emissions. Further decreases in the  $\text{NO}_x/\text{NO}_y$  ratio with  $\text{O}_3$  values between 125 and 300 ppbv were likely because the loss rate of  $\text{NO}_x$  via heterogeneous hydrolysis of  $\text{N}_2\text{O}_5$  is faster for higher  $\text{O}_3$  values. Similar  $\text{O}_3$  dependences of  $d\text{NO}_y$  and  $\text{NO}_x/\text{NO}_y$  values were also seen in the air masses obtained over the U.S. conti-

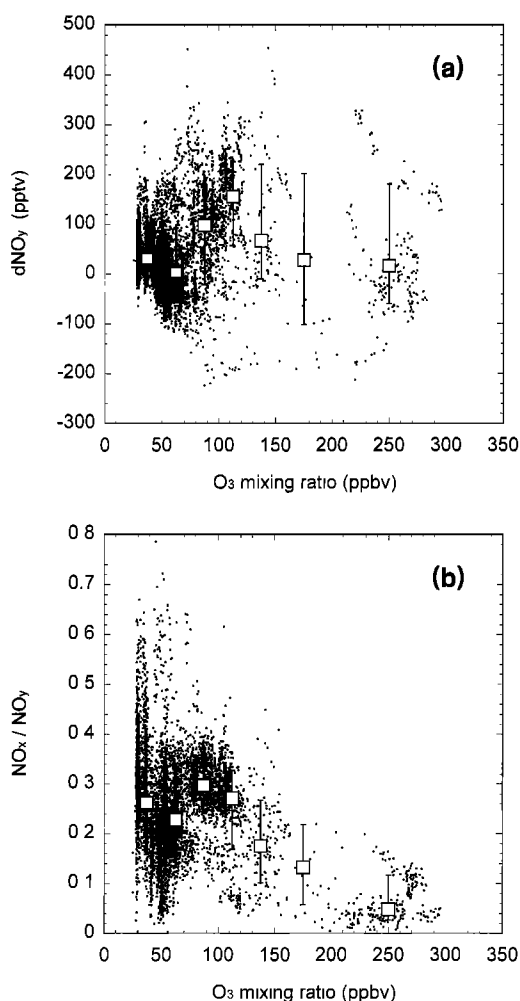


**Figure 13.** Correlation plot between (a)  $d\text{NO}_y$ - $\text{O}_3$  and (b)  $\text{NO}_x/\text{NO}_y$ - $\text{O}_3$  for the data obtained in the NAFC region. The median values and central 67% ranges of the  $d\text{NO}_y$  and  $\text{NO}_x/\text{NO}_y$  ratio are also shown for the seven  $\text{O}_3$  ranges.

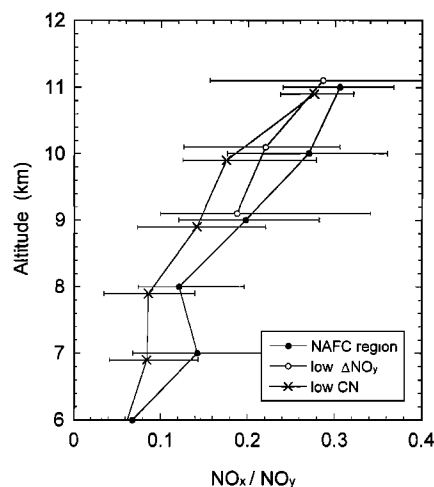


**Figure 14.** Vertical profile of the  $\text{NO}_x/\text{NO}_y$  ratios in the troposphere in the NAFC region (solid circles). The values in the background air masses (open circles: low  $\Delta\text{NO}_y$  (10 days) reference and crosses: low CN reference) are also shown. The median values and central 67% ranges are shown for each 1 km.

nent in the UT and LS. In this case, high  $\text{NO}_x/\text{NO}_y$  ratios of up to 0.3 were observed with  $\text{O}_3$  values as high as 160 ppbv.

### 3.5. Estimation of $d\text{NO}_x$ in the UT

The ratio between excess  $\text{NO}_x$  ( $d\text{NO}_x$ ) and  $d\text{NO}_y$  was estimated from the following expression:

$$\frac{d\text{NO}_x}{d\text{NO}_y} = \left\{ \frac{\text{NO}_x}{\text{NO}_y} - \left( \frac{\text{NO}_x}{\text{NO}_y} \right)_{\text{ref}} \times (1 - \gamma) \right\} \times \frac{1}{\gamma} \quad (1)$$

where  $\gamma = d\text{NO}_y/\text{NO}_y$ . For the reference  $\text{NO}_x/\text{NO}_y$  ratio we used the background air masses that were used to make the reference  $\text{NO}_y$ - $\text{O}_3$  relationship, that is, air masses with  $\Delta\text{NO}_y$  (10 days) values (model  $\text{NO}_x$  input along the 10-day back trajectory) lower than 40 pptv. In Figure 14 a vertical profile of the median  $\text{NO}_x/\text{NO}_y$  ratio in background air masses is shown with that in air masses in the NAFC region. The  $\text{NO}_x/\text{NO}_y$  ratios in the NAFC region were systematically higher than those in the background air masses. Using these  $\text{NO}_x/\text{NO}_y$  values and the  $d\text{NO}_y/\text{NO}_y$  values shown in Table 1 (low  $\Delta\text{NO}_y$  (10 days) reference),  $d\text{NO}_x/d\text{NO}_y$  was calculated for each 1 km altitude level. As a result, the  $d\text{NO}_x/d\text{NO}_y$  ratio was estimated to be 0.54 and 0.38 at altitudes of 10 and 11 km, respectively. Even if the median  $\text{NO}_x/\text{NO}_y$  values in the low CN air masses were used for the reference, similar results were obtained (Figure 14). Furthermore, even if only the data at 45°N–60°N were used for the reference to eliminate a possible effect from the change in the  $\text{NO}_x/\text{NO}_y$  ratio with latitude, similar results were obtained. These results suggest that about half of the excess  $\text{NO}_y$  was likely to be in the form of  $\text{NO}_x$  in the UT. Using an average  $d\text{NO}_x/d\text{NO}_y$  value of 0.46, we found the excess  $\text{NO}_x$  to be 20 and 33 pptv at 10 and 11 km, respectively.

The  $d\text{NO}_x/\text{NO}_x$  ratio can be also expressed using the  $\text{NO}_x/\text{NO}_y$  ratio and  $d\text{NO}_y/\text{NO}_y$  ratio by transforming (1). Using the same values shown above, we estimated that 30% of the  $\text{NO}_x$  at 10 and 11 km was likely to have originated from aircraft emissions in the UT.

#### 4. Summary

The large-scale impact of aircraft emissions on reactive nitrogen in the UT and LS was estimated using the NO<sub>y</sub>-O<sub>3</sub> correlation observed during SONEX, which was carried out over the U.S. continent and NAFC region in October and November 1997. For the present analysis we excluded data obtained within aircraft plumes, data clearly influenced by NO production from lightning, and data influenced by recent convective transport of air affected by surface sources. Two reference NO<sub>y</sub>-O<sub>3</sub> relationships in the air masses, which were considered to be affected little by aircraft emissions, were made using the data obtained above 8.5 km. First, the integrated input of NO<sub>x</sub> into an air mass along a 10-day back trajectory ( $\Delta$ NO<sub>y</sub>) was calculated based on the ANCAT/EC2 aircraft emission inventory. When the  $\Delta$ NO<sub>y</sub> value was less than 40 pptv (lower 42 and 37% values in the UT and LS), that air mass was used for the reference NO<sub>y</sub>-O<sub>3</sub> relationship, irrespective of the location from which it was sampled. Second, air masses with a CN concentration lower than 1500 and 1000 STP cm<sup>-3</sup> (lower 28 and 47% values) in the UT and LS were used to make the reference. Using these two reference NO<sub>y</sub>-O<sub>3</sub> relationships, the two sets of the excess NO<sub>y</sub> ( $d$ NO<sub>y</sub>) were calculated from observed values of NO<sub>y</sub> and O<sub>3</sub>.

The two sets of  $d$ NO<sub>y</sub> values generally agreed within 8 and 18 pptv in the UT and LS, respectively, in spite of the very different nature of the criteria for the background air selection. The calculated  $d$ NO<sub>y</sub> values did not positively correlate with either the CO values or anthropogenically produced hydrocarbons such as C<sub>2</sub>H<sub>2</sub>, suggesting a negligible effect of the surface sources on the  $d$ NO<sub>y</sub> values. On the other hand, the weak positive correlation between the  $d$ NO<sub>y</sub> and  $\Delta$ NO<sub>y</sub> values indicated that the  $d$ NO<sub>y</sub> values generally reflected the effect of aircraft emissions. By calculating the  $d$ NO<sub>y</sub> values only for the air masses which remained over the ocean for 5 days prior to the measurement, the uncertainty in the  $d$ NO<sub>y</sub> values due to the influence of recent NO production by lightning was estimated to be 24%.

In the NAFC region (45°N–60°N) the median value of  $d$ NO<sub>y</sub> in the troposphere was close to zero between 7 and 9 km and increased with altitude above 9 km reaching 70 pptv (20% of NO<sub>y</sub>) at 11 km. High values of  $d$ NO<sub>y</sub> and NO<sub>x</sub>/NO<sub>y</sub> ratio were generally found in air masses in which O<sub>3</sub> = 75–125 ppbv, suggesting a stronger effect around the tropopause. The median value of  $d$ NO<sub>y</sub> in the LS in the NAFC region at 8.5–11.5 km was about 120 pptv. The larger  $d$ NO<sub>y</sub> value observed in the LS was probably the result of the accumulated effect of aircraft emissions, given the long residence time of the affected air in the LS (50 days).

In general, the  $d$ NO<sub>y</sub> value positively correlated with the NO<sub>x</sub>/NO<sub>y</sub> ratio in both the UT and LS in the NAFC and the U.S. continent regions, suggesting that the observed large-scale changes in the NO<sub>x</sub>/NO<sub>y</sub> levels and NO<sub>x</sub> values in the UT and LS were partly caused by NO<sub>x</sub> from aircraft emissions. The slope of the positive correlation between the  $d$ NO<sub>y</sub> and CN values in the LS was generally consistent with that observed in the aircraft plumes, suggesting the importance of aircraft emissions as a source of CN in the LS. A positive correlation between the  $d$ NO<sub>y</sub> and CN values was also seen in a part of air masses in the UT, and its slope was not inconsistent with that observed in the aircraft plumes; however, the significance of aircraft emissions is still not clear.

The ratio between excess NO<sub>x</sub> ( $d$ NO<sub>x</sub>) and  $d$ NO<sub>y</sub> was cal-

culated using the reference NO<sub>x</sub>/NO<sub>y</sub> ratio. In the UT (NAFC region) it was estimated that about half of  $d$ NO<sub>y</sub> was in the form of NO<sub>x</sub> (20 and 33 pptv at 10 and 11 km) and about 30% of the NO<sub>x</sub> had originated from aircraft emissions. These estimates were generally consistent with the results from the model calculations.

In this study, the degree of the large-scale impact of aircraft emissions on reactive nitrogen was estimated from the observed data. A more quantitative estimate will be made using sophisticated three-dimensional models when they can consistently reproduce most of the observed features of various species.

**Acknowledgments.** We are indebted to all of the SONEX participants for their cooperation and support. Special thanks are due to the flight and ground crews of the NASA DC-8 for helping make this effort a success. We thank M. Kanada and H. Jindo for their technical assistance with the measurements of NO and NO<sub>y</sub>. We also thank B. Liley at NIWA, New Zealand, and L. Jaegle at Harvard University for calculating the lifetime of CN and NO<sub>x</sub>, respectively. This work was supported in part by the Ministry of Education, Science, Sports, and Culture.

#### References

- Allen, D., K. Pickering, G. Stenchikov, A. Thompson, and Y. Kondo, A three-dimensional total odd nitrogen (NO<sub>y</sub>) simulation during SONEX using a stretched-grid chemical transport model, *J. Geophys. Res.*, this issue.
- Anderson, B. E., et al., An assessment of aircraft as a source of particles to the upper troposphere, *Geophys. Res. Lett.*, **26**, 3069–3072, 1999.
- Baughcum, S. L., T. Z. Tritz, S. C. Henderson, and D. C. Pickett, Scheduled civil aircraft emissions inventories for 1992: Database development and analysis, *NASA Contract. Rep.*, 4700, 1996.
- Brasseur, G. P., J.-F. Muller, and C. Granier, Atmospheric impact of NO<sub>x</sub> emissions by subsonic aircraft: A three-dimensional model study, *J. Geophys. Res.*, **101**, 1423–1428, 1996.
- Brasseur, G. P., R. A. Cox, D. Hauglustaine, I. Isaksen, J. Lelieveld, D. H. Lister, R. Sausen, U. Schumann, A. Wahner, and P. Wiesen, European scientific assessment of the atmospheric effects of aircraft emissions, *Atmos. Environ.*, **32**, 2329–2418, 1998.
- Clarke, A. D., J. L. Varner, F. Eisele, R. L. Mauldin, D. Tanner, and M. Litchy, Particle production in the remote marine atmosphere: Cloud outflow and subsidence during ACE 1, *J. Geophys. Res.*, **103**, 16,397–16,409, 1998.
- Gardner, R. M. (Ed.), ANCAT/EC2 aircraft emission inventories 1991/1992 and 2015: Final report, Eur. Comm. Working Group, Belgium, 1998.
- Gerz, T., T. Durbeck, and P. Konopka, Transport and effective diffusion of aircraft emissions, *J. Geophys. Res.*, **103**, 25,905–25,913, 1998.
- Gottelman, A., The evolution of aircraft emissions in the stratosphere, *Geophys. Res. Lett.*, **25**, 2129–2132, 1998.
- Hamm, S., G. Helas, and P. Warneck, Acetonitrile in the air over Europe, *Geophys. Res. Lett.*, **16**, 483–486, 1989.
- Holton, J. R., P. H. Haynes, A. R. Douglass, R. B. Rood, and L. Pfister, Stratosphere-troposphere exchange, *Rev. Geophys.*, **33**, 403–439, 1995.
- Jaegle, L., D. J. Jacob, Y. Wang, W. H. Brune, D. Tan, I. C. Faloona, A. J. Weinheimer, B. A. Ridley, T. L. Campos, and G. W. Sachse, Sources of HO<sub>x</sub> and production of ozone in the upper troposphere over the United States, *Geophys. Res. Lett.*, **25**, 17,009–17,012, 1998.
- Klemm, O., W. R. Stockwell, H. Schlager, and H. Zieries, Measurements of nitrogen oxides from aircraft in the northeast Atlantic flight corridor, *J. Geophys. Res.*, **103**, 31,217–31,229, 1998.
- Koike, M., Y. Kondo, S. Kawakami, H. Nakajima, G. L. Gregory, G. W. Sachse, H. B. Singh, E. V. Browell, J. T. Merrill, and R. E. Newell, Reactive nitrogen and its correlation with O<sub>3</sub> and CO over the Pacific in winter and early spring, *J. Geophys. Res.*, **102**, 28,385–28,404, 1997.
- Kondo, Y., H. Ziereis, M. Koike, S. Kawakami, G. L. Gregory, G. W. Sachse, H. B. Singh, D. D. Davis, and J. T. Merrill, Reactive nitro-

- gen over the Pacific Ocean during PEM-West A, *J. Geophys. Res.*, **101**, 1809–1828, 1996.
- Kondo, Y., S. Kawakami, M. Koike, D. W. Fahey, H. Nakajima, N. Toriyama, M. Kanada, Y. Zhao, G. W. Sachse, and G. L. Gregory, The performance of an aircraft instrument for the measurement of NO<sub>y</sub>, *J. Geophys. Res.*, **102**, 28,663–28,671, 1997.
- Kondo, Y., et al., Impact of aircraft emissions on NO<sub>x</sub> in the lowermost stratosphere at northern midlatitudes, *Geophys. Res. Lett.*, **26**, 3065–3068, 1999.
- Lamarque, J.-F., et al., Three-dimensional study of the relative contributions of the different nitrogen sources in the troposphere, *J. Geophys. Res.*, **101**, 22,955–22,968, 1996.
- Mahieu, E., C. P. Rinsland, R. Zander, P. Demoulin, L. Delbouille, and G. Roland, Vertical column abundances of HCN deduced from ground-based infrared solar spectra: Long-term trend and variability, *J. Atmos. Chem.*, **20**, 299–310, 1995.
- Murphy, D. M., D. W. Fahey, M. H. Proffitt, S. C. Liu, K. R. Chan, C. S. Eubank, S. R. Kawa, and K. K. Kelly, Reactive nitrogen and its correlation with ozone in the lower stratosphere and upper troposphere, *J. Geophys. Res.*, **98**, 8751–8773, 1993.
- Pruppacher, H. R., and J. D. Klett, *Microphysics of Clouds and Precipitation*, Kluwer Acad., Norwell, Mass., 1997.
- Ridley, B. A., J. G. Walega, J. E. Dye, and F. E. Grahek, Distribution of NO, NO<sub>x</sub>, NO<sub>y</sub>, and O<sub>3</sub> to 12 km altitude during the summer monsoon season over New Mexico, *J. Geophys. Res.*, **99**, 25,519–25,534, 1994.
- Rinsland, C. P., M. A. H. Smith, P. L. Rinsland, A. Goldman, J. W. Brault, and G. M. Stokes, Ground-based infrared spectroscopic measurements of atmospheric hydrogen cyanide, *J. Geophys. Res.*, **87**, 11,119–11,125, 1982.
- Schlager, H., P. Konopka, P. Schulte, U. Schumann, H. Ziereis, F. Arnold, M. Klemm, D. E. Hagen, P. D. Whitefield, and J. Ovarlez, In situ observations of air traffic emission signatures in the North Atlantic flight corridor, *J. Geophys. Res.*, **102**, 10,739–10,750, 1997.
- Shetter, R. E., and M. Muller, Photolysis frequency measurements using actinic flux spectroradiometry during the PEM-Tropics mission: Instrumentation description and some results, *J. Geophys. Res.*, **104**, 5647–5661, 1999.
- Simpson, I., et al., Nonmethane hydrocarbon measurements in the North Atlantic flight corridor during SONEX, *J. Geophys. Res.*, this issue.
- Singh, H. B., A. M. Thompson, and H. Schlager, SONEX airborne mission and coordinated POLINAT 2 activity: Overview and accomplishments, *Geophys. Res. Lett.*, **26**, 3053–3056, 1999.
- Turman, B. N., and B. C. Edgar, Global lightning distributions at dawn and dusk, *J. Geophys. Res.*, **87**, 1191–1206, 1982.
- Witte, J. C., I. A. Folkins, J. Neima, B. A. Ridley, J. G. Walega, and A. J. Weinheimer, Large-scale enhancements in NO/NO<sub>y</sub> from subsonic aircraft emissions: Comparison with observations, *J. Geophys. Res.*, **102**, 28,169–28,175, 1997.
- Ziereis, H., and F. Arnold, Gaseous ammonia and ammonium ions in the free troposphere, *Nature*, **321**, 503–505, 1986.
- B. E. Anderson, G. L. Gregory, and G. W. Sachse, NASA Langley Research Center, Hampton, VA 23681-0001. (b.e.anderson@larc.nasa.gov; g.l.gregory@larc.nasa.gov; g.w.sachse@larc.nasa.gov)
- D. R. Blake, Department of Chemistry, University California, Irvine, CA 92697. (drblake@uci.edu)
- H. Ikeda, M. Koike, Y. Kondo, N. Toriyama, and Y. Zhao, Solar-Terrestrial Environment Laboratory, Nagoya University, Honohara, Toyokawa, Aichi, 442-8507, Japan. (hibiki@stelab.nagoya-u.ac.jp; koike@stelab.nagoya-u.ac.jp; kondo@stelab.nagoya-u.ac.jp; toriyama@stelab.nagoya-u.ac.jp; yzhao@stelab.nagoya-u.ac.jp)
- K. Kita, Department of Earth and Planetary Physics, Faculty of Science, University of Tokyo, Hongo, Bunkyo-ku, Tokyo, Japan. (kita@grl.s.u-tokyo.ac.jp)
- S. C. Liu, School of Earth and Atmospheric Sciences, Georgia Institute of Technology, 212 Bobby Dodd Way, Atlanta, GA 30332-0340. (shaw.liu@eas.gatech.edu)
- R. E. Shetter, National Center for Atmospheric Research, 1850 Table Mesa Drive, Boulder, CO 80303. (shetter@ncar.ucar.edu)
- H. B. Singh, NASA Ames Research Center, Moffett Field, CA 94035-1000. (hsingh@mail.arc.nasa.gov)
- T. Sugita, National Institute for Environmental Studies, Onogawa, Tsukuba, Ibaraki, 305-0053, Japan. (tsugita@nies.go.jp)
- A. Thompson, NASA Goddard Space Flight Center, Greenbelt Road, Greenbelt, MD 20771-0001. (thompson@gator1.gsfc.nasa.gov)

(Received May 12, 1999; revised September 21, 1999, accepted September 24, 1999.)